Visualization of Cryoballoon Ablation Lesions with 3D LGE Cardiac MR of the Left Atrium

Joseph S Soltys[1], Ibrahim M Saeed[2], Sanjaya Gupta[2], Piero Ghedin[3], Anja C.S. Brau[3], James A Case[1], and Timothy M Bateman[1,2]

[1]*Cardiovascular Imaging Technologies, Kansas City, MO, United States,* [2]*Saint Luke's Mid America Heart and Vascular Institute, Kansas City, MO, United States,* [3]*Global Research Center, GE Healthcare, Munich, Germany*

Purpose: For patients with atrial fibrillation (AF) that is unresponsive to medical therapy a pulmonary vein isolation (PVI) ablation procedure is often successful in restoring normal sinus rhythm. The ablation procedure is traditionally performed with radio-frequency energy to abolish the source of AF[1]. Despite a high short-term success rate for ablation, there is a 27% chance patients have recurrence of AF in the subsequent 10 years[2]. Cardiac MRI is routinely used in the pre-planning of ablation to visualize left atrial and pulmonary vein anatomy[3, 4]. Post RF ablation imaging with cardiac MR has also been reported, however this has primarily been reported using pulse sequences from a single MR platform[3, 4]. Recently, cryoablation has gained popularity as an alternative technique for PVI creating denser and more continuous lesions with better-defined borders[5]. This would make cryoablation induced lesions ideal candidates to be imaged with late gadolinium enhanced (LGE) cardiac MR. It is the purpose of this work to visualize and quantitatively evaluate left atrial cryoablation lesions on a novel cardiac MR platform with commonly available imaging sequences.

Methods: This study was approved by the IRB of Saint Luke's Hospital in Kansas City. Ten consecutive patients (8 M, age 61 ±6 years) who underwent cryoablation for treatment of paroxysmal AF also underwent a cardiac MR post ablation (14 ±7 days) yielding 40 candidate pulmonary veins for analysis. A 3D, IR-prepped, cardiac and respiratory navigated (90-180 NAV signal) fast gradient echo sequence was acquired starting approximately 8-10 minutes after the injection of 0.15 mmol/kg gadobenate dimeglumine. Images were acquired axially with antero-posterior frequency encoding, a typical voxel size of 1.6 x 1.6 x 2.6 mm and adjusted so that the temporal resolution remained below 15% of the RR interval. The scans were performed on a 1.5 Tesla MRI (Signa HDxt, General Electric) with the inversion time selected from an IR prepped multiphase Look-Locker fast gradient echo acquisition prior to the 3D IR prepped NAV scan and adjusted for the expected length of the acquisition.

Only subjects whose follow up cardiac MR was performed at least 21 days post ablation presented visually well characterized lesions, leaving a total of 12/40 pulmonary veins for analysis. Of the 12 remaining pulmonary veins, two (both right inferior) were excluded due to inflow artifact saturating the blood pool signal for a final sample size of 10 pulmonary veins. A cross sectional view at each ablation site as seen on the axial images (Figure 1b) was obtained by multi-planar reformatting until the most complete ring of high signal was visualized along the perimeter (Figure 2) of the pulmonary vein (approximating the position of the cryoballoon). Respective signal intensities for both the ablation lesions and blood pool were recorded using a manually-drawn segmented-line along the enhanced border and a circular ROI at the center of each pulmonary vein cross section using ImageJ (National Institutes of Health). Average completion of each ablation lesion was calculated as the percentage of the ablation lesion line-segment signal greater than the mean of the blood pool plus twice the standard deviation.

Results: A one-sided students T-test with assumed unequal variance indicated that the average observed ablation lesion signal intensity was significantly greater (+16%) than that of the blood pool along the same slice location ($p = 0.004$). An average ablation lesion completion of 58.9 ±17.9% by cryoablation was observed in this study. All patients were followed for an average of 101 days and only 1 patient exhibited a recurrence of AF approximately 9 months after the procedure. The 3 subjects imaged at 21 days post ablation with well-visualized LGE ablation lesions have not demonstrated any clinical evidence of recurrent AF.

Discussion: This analysis identified a significant gadolinium retention signal at the location of each pulmonary vein ablation site. Quantitatively, 7/10 cryoablation lesions examined scored >50% on the two standard deviation criteria. Visually, all subjects had recognizable gadolinium uptake at the cryoablation lesion. Some of the limitations to detect signal were likely due to the loss of resolution in the PVI cross-sections due to use of anisotropic voxel dimensions. Other limitations included the small sample size and the use of a single slice in determining completeness of the PVI.

Conclusion: This study has demonstrated that cryoablation induced lesions can be visualized with cardiac MR using commercially available imaging sequences. On LGE images acquired 3 weeks post cryoablation a hyper-enhancing ring is observed both visually and quantitatively in the majority of pulmonary veins. Additional work is needed to overcome inflow artifact and determine the relationship between the detected LGE ablation ring and the long-term success of the ablation procedure.

Acknowledgements: This study was supported in part by the American College of Cardiology-Missouri Chapter.

References: 1.) Savelieva I, et al. Journal of Interventional Cardiac Electrophysiology 2000;4:369-82. 2.) Steinberg JS, et al. Heart Rhythm 2014;11(5):771-776. 3.) McGann CJ, et al. Journal of the American College of Cardiology 2008;52:1263-71. 4.) Marrouche NF, et al. JAMA 2014;311(5):498-506. 5.) Andrade JG, et al. Circulation: Arrhythmia and Electrophysiology 2013;6:218-227.

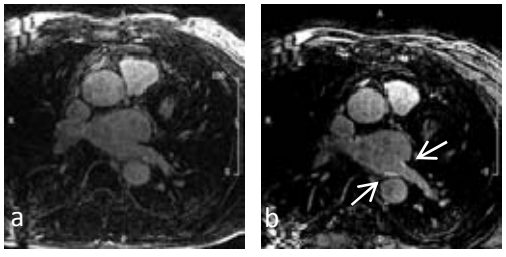

Figure 1. An axial slice of a 3D LGE cardiac MR (a) prior and (b) post cryoablation. Symmetrical lesion is observed on LIPV (arrows).

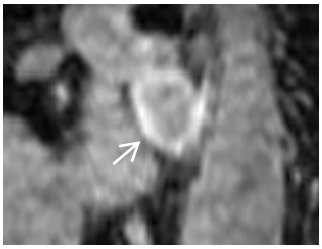

Figure 2. Cross sectional view of PVI at LIPV site indicated on Figure 1b.